New Amphiphilic Rodlike Polymers with Pendent Hemicyanine Groups. 2. Monolayer Behavior

Jung-Hyuk Im, O-Pil Kwon, Jae-Ho Kim, and Suck-Hyun Lee*

Department of Molecular Science and Technology, Ajou University, Suwon, Korea 442-749

Received June 23, 2000; Revised Manuscript Received October 2, 2000

ABSTRACT: Self-assembled monolayers (SAMs) of 2,5-[(*E*)-*N*-methyl-4-[2-[4-[(L)-prolinoxy]phenyl]ethenyl]-pyridinium *p*-toluensulfonate] $(POST)_4$-ester and $POST_4$-amide polymers were prepared on negatively charged solid substrates by the electrostatic interaction between the chromophore and the substrate and characterized using UV−vis spectroscopy, second harmonic generation intensity (SHG) measurement, ellipsometry, and surface-enhanced Raman scattering (SERS) spectroscopy. Simultaneous measurements of UV−vis absorption, SHG intensity, and ellipsometry for the various reaction times indicated that the most densely packed monolayers were found for the two samples. For $POST_4$-ester: reaction time, 30 min; thickness, 12 Å; tilt angle, 34.6°; chromophore density, 3.43/nm^2. For $POST_4$-amide: reaction time, 60 min; thickness, 6 Å; tilt angle, 41.7°; chromophore density, 3.60/nm^2. $POST_4$-amide SAMs showed higher chromophore density and SHG intensity than $POST_4$-ester SAMs due to the intermolecular hydrogen bonding between amide backbones. The order of the second-order susceptibility coefficient, d_{33} was measured to be ca. 400 pm/V for $POST_4$-amide. In situ thermal relaxation studies also revealed high thermal stability. For example, at a high temperature of 120 °C, it was demonstrated that the chromophores inside SAMs were not disorganized but changed in their chemical structure due to the chemical shift of the resonance balance between benzenoid and quinoid forms of the chromophore.

Introduction

The self-assembly of amphiphilic polymers in selective solvents has attracted considerable attention in recent years.[1,2] Monolayer and multilayer formations offer a potential starting point for fabricating highly ordered multifunctional thin films. In particular, assembly of noncentrosymmetric multilayers is a promising technique for preparing second-order nonlinear optical (NLO) films because their noncentrosymmetric structure can be utilized to stabilize the dipole orientation of the NLO chromophore. Nonetheless, this technique often suffers from poor adhesion to substrates and polymer swelling. In addition, chromophore number density and temporal alignment stability are still significant issues in the use of these materials. Our interest in thermally and chemically stable polymeric NLO films via self-assembly has led us to develop materials to incorporate hemicyanine salt units as pendent side chains in rigid backbone polymers. The strategy of increasing the content and orientational order of chromophores utilizing wholly aromatic polymers as rigid backbones helps reduce aggregation and simultaneously provides a highly ordered environment for the chromophores. To the best of our knowledge, monolayer preparation by the simple adsorption of amphilphilic side chain chromophores based on rigid backbone polymers has not yet been reported in the literature. Adsorption by rigid-chain polyelectrolytes to a charged surface may be of interest for understanding the screening effect of charge interactions in polymeric systems because the rigid chains retain their extended conformation regardless of the ionic strength. In the preceding paper, we described the synthesis of wholly aromatic polymers bearing hemicyanine salt units in the side chain and investigated their properties including optical nonlinearity. The polymers have the following structures.

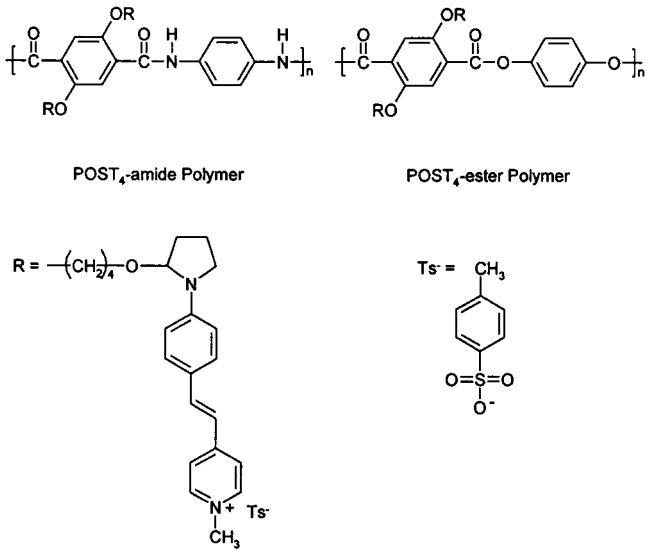

These polymers were soluble in both of the protic and aprotic solvents and exhibited polyelectrolyte behavior in deionized water. Significant second harmonic generation (SHG) activity was observed from the spin-coated films without the aid of electric field induced poling. However, the bulk susceptibility of corona-poled films was found to be smaller than expected due to the inefficient electric poling. We now describe the preparation of monolayers from these polymers. The main objective is to determine whether the rigid chain amphiphiles deposit onto hydrophobic silicon wafers to give stable monolayers in order to eventually construct multilayers by a consecutive adsorption of polyanions and polycations with asymmetric structures. Characterization results for these monolayers using UV−vis spectrometry, ellipsometry, SHG technique, and surface-enhanced Raman scattering (SERS) spectroscopy, aimed

10.1021/ma0010940 CCC: $19.00
Published on Web 11/30/2000

at demonstrating the success of the highly stable monolayer formation, are discussed in this paper.

Experimental Section

Materials. The polymers used here, $POST_4$-ester and $POST_4$-amide, were prepared by the solution polycondensation reaction. The details on the syntheses and their characterizations were described in the preceding paper. The number-average molecular weights of both polymers were on the order of 10^4. The T_g of the polymers, $POST_4$-ester and $POST_4$-amide are 80 and 139 °C, respectively. All chemicals such as sulfuric acid, hydrogen peroxide, aqueous ammonia were purchased from J. T. Baker. The ultrapure water used for all cleaning steps and as solvent for adsorption was obtained by ion-exchanged and filtration system (Milli-Q, Millipore GmbH). The resistivity was better than 18 MΩ•cm. Glass slides were obtained from Gebruder Rettgerg.

Preparation of Self-Assembled Films. Glass slides and silicon wafers (for ellipsometric measurements) were used as substrates for the self-assembly. These substrates were washed for 30 min in a solution containing 30% in a mixture of water/methanol (3:7) to remove some organic impurities on surface, and the substrates were retreated to give rise to more hydrophilic property by immersion into "piranha solution" (7:3 concentrated H_2SO_4/30% H_2O_2) at 80 °C for 30 min. After treating, the substrates were washed in Milli-Q water many times and dried with an N_2 gas stream. The adsorption was carried out as follows. Hydrophilic treated substrates were immersed into 1 mM aqueous $POST_4$-ester and $POST_4$-amide solution at room temperature for various times, respectively. After deposition of polymeric monolayer, the substrates were thoroughly rinsed three times in pure water and dried with a N_2 gas stream.

UV−Vis Spectroscopy. A JASCO V-550 UV/vis spetrophotometer (Japan Spectroscopic Co., Tokyo, Japan), working in the range 190−850 nm, with a resolution of 0.5 nm per element, was used to obtain UV−vis spectra of each polymeric solution and self-assembled (SA) films. All spectra were recorded after baseline correction.

Ellipsometry. Ellipsometric measurements were carried out on a variable-angle spectroscopic ellipsometer (VASE) system (J. A. WOOLLAM Co., Inc, NE) using a wavelength of 632.8 nm (He−Ne laser). Ellipsometric ψ and Δ data were acquired at three angles of incidence (65, 70, and 75°) over the spectral range 300−1000 nm in steps of 20 nm and were analyzed using WVASE 32 software version 3.255. To determine the accurate thickness of the SA monolayer, a bare Si wafer was provided for an oxide reference measurement. This oxide thickness, 19.65 Å, was held fixed when fitting for each SA sample. The refractive index was taken from the spin-coated thick film and not allowed to vary. From the result, the refractive indices of the SAM on glass were measured as $n^{2w} = 1.55$ and $n^{w} = 1.46$.

Second Harmonic Generation. The NLO properties of the SA monolayer films were investigated using SHG measurements in the transmission geometry. The SHG measurements were made using a Q-switched Nd:YAG laser operating at 1064 nm with a pulse repetition rate of 10 Hz. The pulse energy was 0.45 mJ. The sample was rotated using Oriel stepper moter with resolution of 0.1°, allowing the angle of incidence to be varied from 0 to 90°. The transmitted SHG signal at 532 nm was separated from the fundamental beam using infrared cut filter and detected by the photomultiplier tube (Oriel 7070). A quartz crystal was used as the reference.

Surface-Enhanced Raman Scattering (SERS) Spectroscopy. SERS spectra were collected using a triple monochromator coupled with a blue intensified CCD array detector (Triplemate 1877, Spex Industries, Edison, NJ). The excitation source was 514.5 nm line of an Ar^+ laser (INNOVA 70−5, Coherent Co., Santa Clara, CA) with 10 mW at the sample. The angle of the laser excitation source was ∼45° with respect to the surface normal, and Raman scattered light was collected parallel to the surface normal. Ag colloidal film, having average particle size of 60 nm, was used as a SERS active substrate. The procedure constructing Ag colloidal solution and film was described in detail in the literature.[3]

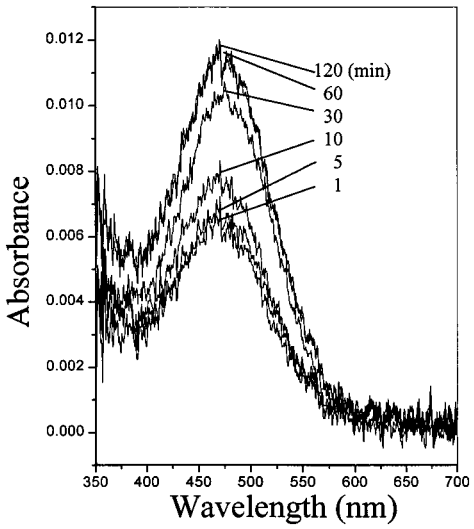

Figure 1. UV−vis absorption spectra of $POST_4$-ester as a function of reaction time during SAM formation on glass substrate. The λ_{max} value is 473 nm in the initial state and does not change with reaction time.

Results and Discussion

The adsorption process of monolayers is strongly affected by the ability of molecules to pack at the interface, and this is directly linked to molecular conformation and intermolecular interactions. We used cationic hemicyanine groups introduced into two backbone polymers, namely $POST_4$-ester and $POST_4$-amide, for the preparation of the monolayers. We expected the latter polymer to pack more efficiently on the surface due to their intermolecular hydrogen-bonding capability. Indeed the results indicated a significant enhancement of the optical nonlinearity and thermal stability for this polymer.

Monolayer Preparation. We studied changes in molecular organization on dipping time during the preparation of monolayers of the two samples by means of UV−vis spectrophotometry and SHG intensity measurement. Figures 1 and 2 show the self-assembly monitored by the absorption of the transmitted UV−vis light. Glass-supported films exhibited an absorption peak at 475 nm due to the NLO chromophore, and no new bands at different wavelengths appeared relative to the initial spectra, suggesting negligible formation of dipole aggregates. This observation is consistent with their attachment to the rigid backbone polymers. Figure 3 shows that the absorbance increases almost linearly with dipping time and then saturates for $POST_4$-ester. However, the absorbance rise in $POST_4$-amide apparently occurs in two steps: an initial fast rise in absorbance followed by a slow rise (Figure 4). Comparison of the transients shows also that the intensity rise in $POST_4$-ester approaches the asymptote at a faster rate. This difference could be attributed to the difference in the structure and conformation of the polymer backbone. We think that the complexation between charged substrate and polymer proceeds in two steps: the first step is a simple complexation without registry of the substrate pattern and the second step is a process of registry. When the surface contains many polyelectrolyte chains attached to an oppositely charged surface, some of the ionic pairs must dissociate and reassociate

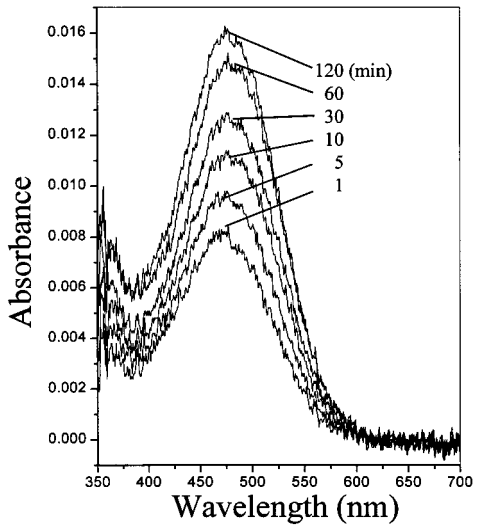

Figure 2. UV−vis absorption spectra of $POST_4$-amide as a function of reaction time during SAM formation on glass substrate. The λ_{max} value is 474 nm in initial state and slightly red-shifted with the reaction time, 478 nm at 60 min.

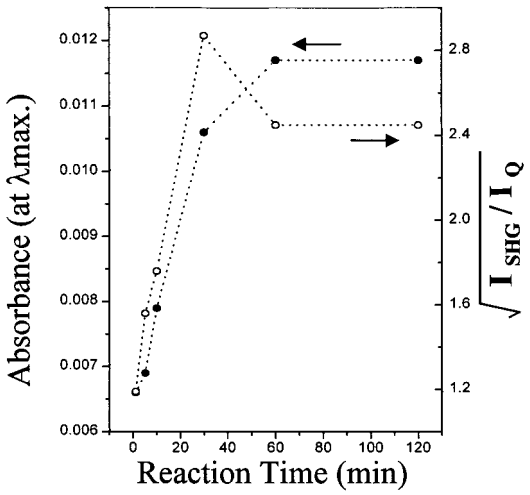

Figure 3. Plots of the absorbance change at λ_{max} and $I_{SHG}^{1/2}$ values for $POST_4$-ester with the reaction time. Maximum SH intensity is observed at the reaction time of 30 min.

differently in a cooperative manner to proceed with complete adsorption so as to achieve the final minimum free energy structure. These restrictions on the pathways connecting different topological states prolong the second step of adsorption. We believe that this second process of the recognition of a specific substrate pattern in the case of the $POST_4$-amide is much slower due to the greater contour length and the resulting longer range of stronger intermolecular interactions. In fact, we observed that the solution viscosity in pure water was larger for $POST_4$-amide compared to $POST_4$-ester at the same concentration, indicating a greater contour length.

NLO Properties. SHG methods are sufficiently sensitive to detect chromophore alignments in ultrathin films. The SHG was investigated during the preparation of the monolayer in transmission geometry at an incidence angle of 45°. Figures 3 and 4 show that the measured SHG intensity, $I_{shg}^{1/2}$ against the reaction times for the two samples. $I_{shg}^{1/2}$ was used here to compare the surface coverage of the chromophores because the second-order nonlinear susceptibility coefficient d depends on the number of chromophores per unit volume and I_{shg} is related to d^2. The observed SHG behaviors for $POST_4$-amide were different from the absorbance data. The SHG intensity increased and then decreased showing a maximum in contrast with a steady increase in absorbance. Further, the SHG intensity for $POST_4$-ester grew almost linearly and then leveled off whereas it decreased rapidly after the initial two-step growing for $POST_4$-amide. This difference is probably due to polar ordering of the chromophores by way of the dipole reversal in double-layering process, the SHG being canceled by the centrosymmetric alignment in such regions of the film. Because the adsorption is driven by the ionic bonds of the hemicyanine groups, it should lead to a noncentrosymmetric orientation layer of the chromophores and thus to a second-order NLO response of the layer, on which a hydrophobic layer of the polymer backbones is overlayed. Given this hydrophobic layer of the backbone polymers, a double layer can be constructed by intermolecular interaction of the hydrophobic backbone chains with the ionic chromophores arranged with their polar axes in the reverse direction of the chromophores in the monolayer. Such molecular interaction dominates relative to the monolayer-substrate interaction after complete adsorption, resulting in a maximum in the SHG data. This layering seems to be particularly relevant to the polyamide backbone whose intermolecular hydrogen bond favors attractive interaction between the polymer backbones. Therefore, it is obvious from these figures that the drop of the SHG signal arises with the occurrence of a double layer. The thickness of the monolayer measured by ellipsometry corroborates the formation of an additional layer by a consecutive adsorption of polymer backbones. As shown in Figure 5, the thickness increases and eventually reaches its stable level of ca. 12 Å after half an hour of reaction for $POST_4$-ester whereas it starts to increases again after a short level of steady state for $POST_4$-amide. The latter growth pattern indicates clearly that a monolayer of ca. 9 Å thickness was formed in an hour of reaction and then a double layer began to grow on further reaction.

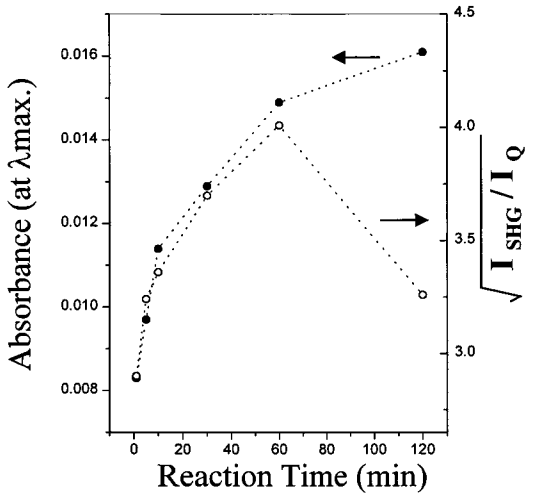

Figure 4. Plots of the absorbance change at λ_{max} and $I_{SHG}^{1/2}$ values for $POST_4$-amide with the reaction time. Maximum SH intensity is observed at the reaction time of 60 min.

Now we discuss the orientation of the chromophores in polar self-assembled monolayers. Assuming that the chromophores have a common tilt angle with respect to the surface normal and that the molecular hyperpo-

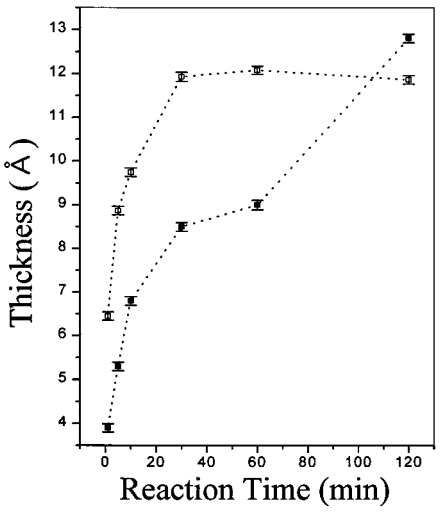

Figure 5. Plots of estimated thickness as a function of the reaction time for both samples: $POST_4$-ester (□); $POST_4$-amide (■).

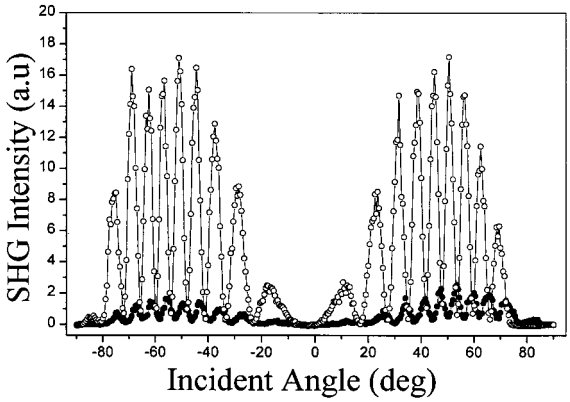

Figure 6. Transmitted SHG intensity at 532 nm as a function of the incident angle of the polarized light. The data were taken from the sample of $POST_4$-amide SAM with the reaction time of 60 min: p−p polarization (○); s−p polarization (●).

larizability is dominated by the component along the molecular axis only, we can estimate the chromophore tilt angle from the polarized SHG response. Figure 6 shows a typical SHG interference pattern from a substrate with a monolayer film on both surfaces for the p- and s- polarized fundamentals at 1064 nm. The interference fringes of the SHG intensity arise from the interaction of the second-harmonic waves from the samples on both sides of the substrate.[4,5] The fairly smooth envelope was obtained as the film was rotated from the normal incidence to grazing incidence. Any azimuthal orientation dependence was not detected, however when rotation within the plane of the film was carried out, indicating uniaxial symmetry of the homogeneous films about the surface normal.[6] We attempted to determine the second-order NLO susceptibility, d_{33} by curve fitting of this envelope according to a theoretical model but the result was not satisfactory. The experimental data systematically deviated from the theoretical values and χ^2, and the value of the good fit was 3.9. However, the calculation at a peak angle of the Maker fringe by comparison with the peak signal from the quartz reference of 1 mm thick (d_{11}, 0.3 pm V^{-1}) resulted in a very large value of 400 pm V^{-1} for $POST_4$-amide. Note that the d_{33} value of this monolayer at 532 nm was estimated to be 580 pm V^{-1}, calculated from

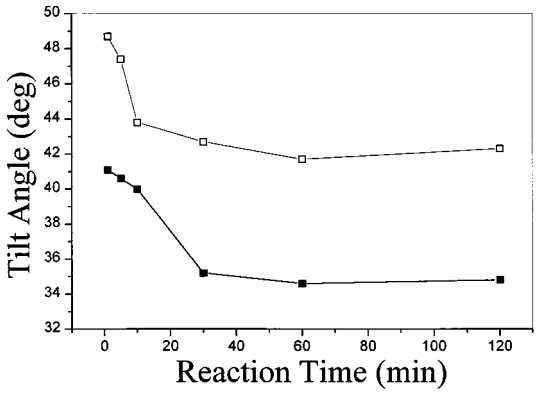

Figure 7. Plots of the tilt angle of chromophore to the surface normal as a function of reaction times: $POST_4$-ester (■); $POST_4$-amide (□).

the oriented gas approximation. The large nonlinearity can be caused by several factors that have an influence on the susceptibility of a polymer: the chromophore number density, the order parameter of the monolayer, and the enhancement due to resonance absorption. Some resonance enhancement cannot be ruled out even in ultrathin films, but the observed large NLO response is probably a direct result of highly dense chromophores with minimal dipole pairing due to attachment at the rigid chain in the monolayer. We will discuss the surface coverage of the chromophores in the monolayer later.

Tilt Angle. By comparing the SH signal intensity from p-polarized excitation wave with s-polarized excitation one, we obtained the average tilt angle from eq 1.[7−9] As shown in Figure 7, the tilt angle decreased

$$\tan \phi = [(I^{p-p}{}_{2\omega}/I^{s-p}{}_{2\omega})^{1/2} - 3/2]^{-1/2} \qquad (1)$$

initially with the reaction time and eventually stabilized, indicating that highly ordered structures formed with a net alignment as the surface coverage increased. The optimized alignment was found as being tilted at angles of ca. 35 and 41° from the surface normal for $POST_4$-ester and $POST_4$-amide, respectively. We think that these values of the tilt angle are reliable because their evaluation was performed independent of complicating factors such as the local field effects.

Surface Coverage. Since the chromophore molecule strongly absorbs UV−vis light, the absorbance of the monolayer can be used to determine the surface coverage, $d_{surf} = A\epsilon^{-1}$. First, we utilized the absorptivity of the chromophore in the monolayer for light polarized parallel to the surface, A_{surf}, as well as the measured tilt angle to deduce the extinction coefficient for the same number of identical species in solution, A_{soln} from eq 1.[10,11]

$$\sin^2<\Phi> = 2A_{surf}/3A_{soln} \qquad (2)$$

The surface density of the chromophore was then calculated in units of molecules per nm^2 using the above extinction coefficient with a surface area measured by AFM for both samples. The extinction coefficient of the chromophore is 1.18×10^7 cm^2/mol in aqueous solution. The surface area of the substrate after hydrophilic treatment was calculated in terms of projected area from 100 nm^2 sized AFM image. Tables 1 and 2 show the determined values for $POST_4$-ester and $POST_4$-amide, respectively. The estimated surface coverages, molecular

Table 1. Main Characteristics of $POST_4$-ester SAM

reacn time (min)	1	5	10	30	60	120
λ_{max} (nm)	473	473	473	473	473	473
A_{surf} at 473 nm	0.0066	0.0069	0.0079	0.0106	0.0117	0.0117
SHG intens (au)	1.41	2.44	3.09	7.74	6.01	6.02
I^{p-p}/I^{s-p} at 45°	7.9	8.2	8.5	12.3	13	12.8
A_{soln}(calcd)	0.0102	0.0109	0.0128	0.0213	0.0242	0.0239
tilt angle (deg)	41.1	40.6	40.0	35.2	34.6	34.8
Γ_{surf} ($\times 10^{-10}$)	8.64	9.24	10.8	18.1	20.5	20.2
molecules/1 nm^2	1.64	1.75	2.05	3.43	3.89	3.83
thickness (Å)	6.4	8.8	9.7	11.9	12.1	11.7

Table 2. Main Characteristics of $POST_4$-amide SAM

reacn time (min)	1	5	10	30	60	120
λ_{max} (nm)	474	476	477	478	478	477
A_{surf} at λ_{max}	0.0083	0.0097	0.0114	0.0129	0.0149	0.0161
SHG intens (au)	8.4	10.5	11.3	13.7	16.1	10.6
I^{p-p}/I^{s-p} at 45°	5.2	5.5	6.7	7.15	7.61	7.31
A_{soln}(calcd)	0.0098	0.0119	0.0159	0.0187	0.0224	0.0237
tilt angle (deg)	48.7	47.4	43.8	42.7	41.7	42.3
Γ_{surf} ($\times 10^{-10}$)	8.31	10.1	13.5	15.8	19.0	20.1
molecules/1 nm^2	1.58	1.92	2.56	3.00	3.60	3.81
thickness (Å)	3.9	5.3	6.8	8.5	9.0	12.8

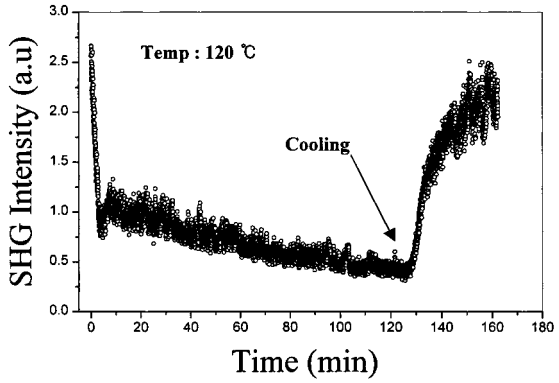

Figure 8. In situ SHG intensity change for $POST_4$-amide (reaction time: 60 min) with the time at 120 °C. After keeping the sample at 120 °C for ca. 130 min, it is cooled in air until the temperature reaches 23 °C.

packing densities of 3.43 and 3.60/nm^2, approached a close-packed state, indicating that the monolayers are densely packed.[11,12] The observed red shift and broadening of the charge-transfer band also supports intermolecular close packing of the chromophores (Figures 1 and 2). It is interesting also to point out that the packing density of $POST_4$-amide was significantly higher than that of $POST_4$-ester. When rodlike backbone polymers were forced together, steric hindrance acted on the chains to give rise to their spontaneous alignment. The resulting hydrogen-bonding interactions of adjacent backbone molecules leads to denser packing in polyamide sample. The following absorption spectroscopic results confirmed this: The red-shift of ca. 4 nm at λ_{max} occurred in $POST_4$-amide SAM with the reaction time, while no change was found in $POST_4$-ester SAM. We believe that the hydrogen-bonding interaction of backbones in $POST_4$-amide SAM allows the reorganization of chromophores between polymer chains to give rise to J-like aggregation on surface.

Thermal Stability. To probe the thermal stability of the monolayer, we monitored the temporal stability of the SHG signal at high temperatures. Typical results are depicted in Figure 8. Upon heating to 120 °C, a large decay occurred during the first few minutes and thereafter gradual decay was observed for more than 2 h. Of particular interest in this figure is the fact that the SHG

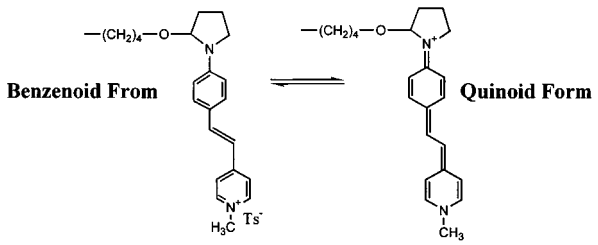

Figure 9. Resonance electric balances of hemicyanine chromophore between benzenoid and quinoid forms.

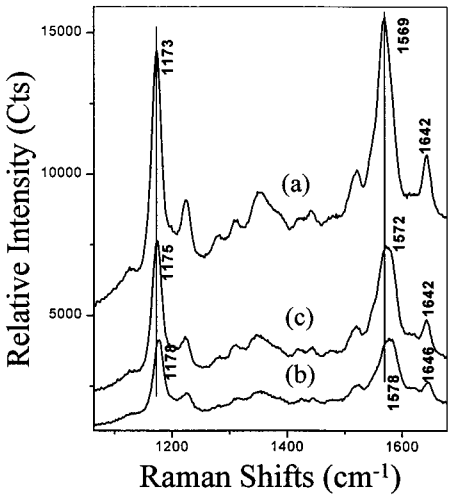

Figure 10. In situ SERS spectra of $POST_4$-amide SAM (reaction time: 60 min) on negatively charged Ag colloidal film. Excitation wavelength and power, 514.5 nm (Ar^+ laser), 10 mW at sample: (a) at 23 °C, (b) at 120 °C, 60 min, and (c) at 23 °C, after cooling.

signal recovers rapidly when the temperature decreased to nearly the initial value. When this process was repeated for the sample after complete recovery, data similar to that shown in Figure 8 was obtained. To our knowledge this is the first time the SHG recovery is observed for the NLO sample subjected to a thermal relaxation treatment. Since the ionic chromophore is adsorbed onto the substrate surface, the observed SHG decay is not consistent with either realignment of the dipole groups or randomization of backbone arrangement at this temperature. On the basis of reversible change, we expected that the decay would be related to the chemical shift of the resonance balance between benzenoid and quinoid forms caused by thermal energy at high temperatures. Figure 9 depicts the chromophore in its two resonance states upon thermal excitation. If this chemical change is indeed the cause of the SHG change, the central C=C stretching mode of the chromophore can be used to detect the shift. Figure 10 shows surface-enhanced Raman scattering spectra for three samples with different thermal history. The useful probes are scattering bands at 1573 and 1173 cm^{-1} assigned to a stretching mode of the central C=C bond and to a symmetric stretching mode of the two C−C bonds connecting the phenyl and pyridyl groups and the C=C bond,[13] respectively. The frequency lowering of the former peak from 1578 to 1569 cm^{-1} indicates the increase in the contribution of the quinoid form because the bond order of the central C=C of the quinoid form is lower than that of the benzenoid form.[14] To emphasize similar trends, UV−vis spectra for the same samples are also presented in Figure 11. The observed red shift

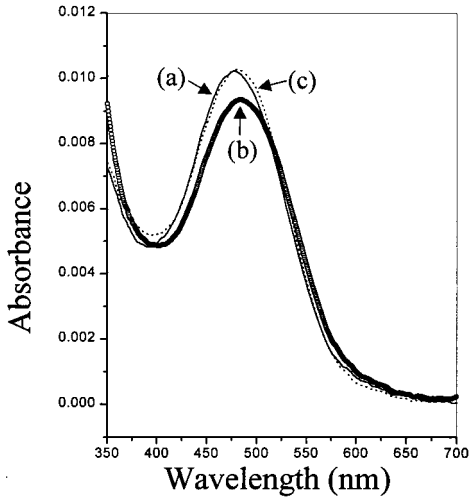

Figure 11. In situ UV−vis spectra of $POST_4$-amide SAM on glass substrate: (a) at 23 °C, (b) at 120 °C, 60 min, and (c) at 23 °C, after cooling. The λ_{max} are (a) 477, (b) 485, and (c) 480 nm.

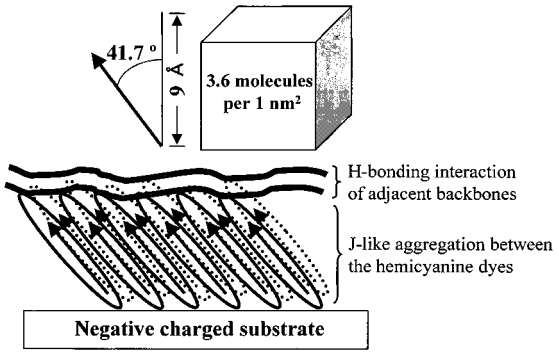

Figure 12. Schematic diagram of an aggregation mode for $POST_4$-amide (reaction time: 60 min) on negatively charged substrate.

indicates the chemical change of the chromophore. In view of the above observations, we have attributed the drop-off in the SHG signal to the chemical change of NLO chromophores rather than to the dipolar realignment. The slow decay of the remaining SHG signal is probably associated with the equilibrium between the two forms. As the equilibrium is approached the SHG signal gradually decreases to zero level due to the complete dipolar pairing. Despite this chemical instability of the chromophore, this result is encouraging because it shows that the monolayer itself is very stable even at the high temperature of 120 °C. We believe that the strong intermolecular interaction of the backbones along with the formation of inherently stable noncentrosymmetric structures in the monolayer overcomes the tendency of the chromophores to relax to thermodynamically more stable orientation isotropy. The present new amphiphilic polymers based on hydrophobic rigid backbones would offer high potential in the self-assembly field. A schematic diagram of such an aggregation mode for POST4-amide is presented in Figure 12.

Conclusion

We have clearly demonstrated that self-assembled monolayers are well constructed from the amphiphilic polymers based on the hydrophobic rigid backbone polymers. By measuring simultaneously UV−vis absorption and SHG intensity, we have found that the densely packed monolayers of thicknesses ca. 12 and 9 Å were formed for the two samples, $POST_4$-ester and $POST_4$-amide, respectively. The order of the second-order susceptibility coefficient, d_{33} was measured to be 400 pm/V for $POST_4$-amide. By monitoring the SHG, SERS and UV−vis spetra at high temperature, it was demonstrated that the monolayer itself was very stable at such high temperatures even though the decay in the SHG occurred due to the chemical shift of the resonance balance between benzenoid and quinoid forms of the chromophore. The materials based on the polyamide backbone yielded better NLO properties and thermal stability than the analogous polyester based materials, which was attributed to the more rigid backbone and intermolecular hydrogen-bonding effect.

Acknowledgment. S.H.L. is thankful for financial support by the Korea Science and Engineering Foundation through the Hyperstructured Orgaic Materials Research Center.

References and Notes

(1) Decher, G. *Science* **1997**, *277*, 1232.
(2) Moriguchi, I.; Teraoka, Y.; Kagawa, S.; Fendler, J. H. *Chem. Mater.* **1999**, *11*, 1603.
(3) Park, S. H.; Im, J. H.; Im, J. W.; Chun, B. H.; Kim, J. H. *Microchem. J.* **1999**, *63*, 71.
(4) Johal, M. S.; Parikh, A. N.; Lee, Y.; Casson, J. L.; Foster, L.; Swanson, B. I.; McBranch, D. W.; Li, D. Q.; Robinson, J. M. *Langmuir* **1999**, *15*, 1275.
(5) Li, D. Q.; Swanson, B. I.; Robinson, J. M.; Hoffbauer, Ma. *J. Am. Chem. Soc.* **1993**, *115*, 6975.
(6) Li, D.; Ratner, M. A.; Marks, T. J.; Zhang, C.; Yang, J.; Wang, G. K. *J. Am. Chem. Soc.* **1990**, *112*, 7389.
(7) Kajikawa, K.; Kigata, H.; Takezoe, H.; Fukuda, A. *Mol. Cryst. Liq. Cryst.* **1990**, *182*, 91.
(8) Ashwell, G. J.; Hargeaves, R. C.; Baldwin, C. E.; Bahra, G. S.; Brown, C. R. *Nature* **1992**, *357*, 393.
(9) Ashwell, G. J.; Ranjan, R.; Whittam, A. J.; Gandolfo, D. S. *J. Mater. Chem.* **2000**, *10*, 63.
(10) Buscher, C. T.; McBranch, D.; Li, D. *J. Am. Chem. Soc.* **1996**, *118*, 2950.
(11) Moon, J. H.; Kim, J. H.; Kim, K. J.; Kang, T. H.; Kim B. S.; Kim, C. H.; Hahn, J. H.; Park, J. W. *Langmuir* **1997**, *13*, 4305.
(12) Wolf, H.; Ringsdorf, H.; Delamarche, E.; Takami, T.; Kang, H.; Michel, G.; Gerber, C. H.; Taschke, M.' Butt, H. J.; Bamberg, E. *J. Phys. Chem.* **1995**, *99*, 7102.
(13) Tsukada, M.; Mineo, Y.; Itoh, K. *J. Phys. Chem.* **1989**, *93*, 7989.
(14) Shibasaki, K.; Itoh, K. *J. Raman Spectrosc.* **1991**, *22*, 753.

MA0010940